



Published in final edited form as:

*Circ Arrhythm Electrophysiol.* 2017 April ; 10(4): . doi:10.1161/CIRCEP.116.004937.

## Premature Ventricular Contraction Coupling Interval Variability Destabilizes Cardiac Neuronal and Electrophysiological Control: Insights from Simultaneous Cardio-Neural Mapping

David Hamon, MD<sup>1,2,\*</sup>, Pradeep S. Rajendran, BS<sup>1,2,3,\*</sup>, Ray W. Chui, MS<sup>1,2,3</sup>, Olujimi A. Ajijola, MD, PhD<sup>1,2</sup>, Tadanobu Irie, MD, PhD<sup>1,2</sup>, Ramin Talebi, BS<sup>1,2</sup>, Siamak Salavatian, PhD<sup>1,2</sup>, Marmar Vaseghi, MD, PhD<sup>1,2,3</sup>, Jason S. Bradfield, MD<sup>1</sup>, J. Andrew Armour, MD, PhD<sup>1,2</sup>, Jeffrey L. Ardell, PhD<sup>1,2,3</sup>, and Kalyanam Shivkumar, MD, PhD<sup>1,2,3</sup>

<sup>1</sup>University of California – Los Angeles (UCLA) Cardiac Arrhythmia Center, David Geffen School of Medicine, UCLA, Los Angeles, CA

<sup>2</sup>Neurocardiology Research Center of Excellence, David Geffen School of Medicine, UCLA, Los Angeles, CA

<sup>3</sup>Molecular, Cellular & Integrative Physiology Program, David Geffen School of Medicine, UCLA, Los Angeles, CA

### Abstract

**Background**—Variability in premature ventricular contraction (PVC) coupling interval (CI) increases the risk of cardiomyopathy and sudden death. The autonomic nervous system regulates cardiac electrical and mechanical indices, and its dysregulation plays an important role in cardiac disease pathogenesis. The impact of PVCs on the intrinsic cardiac nervous system (ICNS), a neural network on the heart, remains unknown. The objective was to determine the effect of PVCs and CI on ICNS function in generating cardiac neuronal and electrical instability using a novel cardio-neural mapping approach.

**Methods and Results**—In a porcine model (n=8) neuronal activity was recorded from a ventricular ganglion using a microelectrode array, and cardiac electrophysiological mapping was performed. Neurons were functionally classified based on their response to afferent and efferent cardiovascular stimuli, with neurons that responded to both defined as convergent (local reflex processors). Dynamic changes in neuronal activity were then evaluated in response to right ventricular outflow tract PVCs with fixed short, fixed long, and variable CI. PVC delivery elicited a greater neuronal response than all other stimuli (P<0.001). Compared to fixed short and long CI, PVCs with variable CI had a greater impact on neuronal response (P<0.05 versus short CI), particularly on convergent neurons (P<0.05), as well as neurons receiving sympathetic (P<0.05) and parasympathetic input (P<0.05). The greatest cardiac electrical instability was also observed following variable (short) CI PVCs.

Correspondence: Kalyanam Shivkumar, MD, PhD, UCLA Cardiac Arrhythmia Center, 100 Medical Plaza, Suite 660, Los Angeles, CA 90095, Tel: 1-310-206-6433, Fax: 1-310-794-6494, kshivkumar@mednet.ucla.edu.

\*contributed equally

**Disclosures:** None.

**Conclusions**—Variable CI PVCs affect critical populations of ICNS neurons and alter cardiac repolarization. These changes may be critical for arrhythmogenesis and remodeling leading to cardiomyopathy.

### Journal Subject Terms

Autonomic Nervous System; Pathophysiology

### Keywords

premature ventricular beats; coupling; autonomic nervous system; neurocardiology; intrinsic cardiac ganglia; PVC-induced cardiomyopathy

---

## Introduction

Premature ventricular contractions (PVCs) are common in clinical practice. In structurally normal hearts, despite being referred to as “benign”, PVCs may lead to cardiomyopathy (CMP)<sup>1</sup> or even to sudden cardiac death.<sup>2, 3</sup> Recent clinical studies have identified factors that predict worse outcomes in PVC patients. Particularly, patients with PVCs showing high coupling interval (CI) variability are at a greater risk for cardiac events such as left ventricular (LV) dysfunction<sup>4</sup> and sudden cardiac death.<sup>5, 6</sup>

Precise mechanisms underlying the adverse effects of PVCs remain unknown, but are likely multifactorial including mechanical dyssynchrony,<sup>7, 8</sup> abnormalities in calcium handling and oxygen consumption,<sup>9</sup> and autonomic imbalance.<sup>10</sup> Of these mechanisms, the role of the autonomic nervous system (ANS) is not well understood. The ANS regulates all aspects of cardiac function.<sup>11</sup> Afferent sensory neurons provide beat-to-beat information regarding the cardiac milieu. Processing and integration of this information at different levels of the ANS, including the intrinsic cardiac nervous system (ICNS), provides an elegant mechanism to ensure fine-tuned regulation of efferent neural signals to the heart.<sup>11</sup> The ICNS, a distributed network of ganglia and interconnecting nerve fibers on the epicardial surface, represents the first level of the ANS directly impacted by cardiac injury.<sup>12–14</sup> Even in normal states, disruptions of ICNS function are arrhythmogenic.<sup>15</sup> Moreover, neural remodeling within the ICNS following cardiac injury has been correlated with arrhythmias.<sup>11, 14</sup>

As both PVCs with variable CI and the ICNS have been linked to CMP and life-threatening arrhythmias, we hypothesized that variability in PVC CI could induce destabilizing changes in the ICNS. Therefore, the purpose of this study was to evaluate in an *in vivo* porcine model the impact of PVC CI on: (1) intrinsic cardiac neuronal activity and (2) cardiac electrical and mechanical parameters using a novel cardio-neural mapping approach that utilizes direct neuronal recordings from a beating heart.

## Methods

Expanded version of Methods are presented in the online-only Data Supplement.

## Animals

Eight Yorkshire pigs (5 male and 3 female, weighing  $57.1 \pm 2.5$  kg) were used in this study. Animal experiments were performed in accordance with the National Institute of Health's Guide for the Care and Use of Laboratory Animals and approved by the University of California, Los Angeles Chancellor's Animal Research Committee.

## Hemodynamic assessment

LV cardiac mechanical indices were continuously recorded and analyzed at baseline and following interventions including each of the PVC types.

## Heart rate variability

Heart rate variability at baseline and following each of the PVC types was analyzed using the software Acknowledge (Biopac Systems, Goleta, CA, USA).

## Experimental protocol

After animals stabilized following surgical preparation, cardiac neuronal activity was identified and the following protocol was performed. Hemodynamic indices, cardiac electrophysiological data, and neuronal activity were recorded at baseline and during 5 minutes of PVCs and premature atrial contractions (PACs). PVCs and PACs were delivered every 10-sensed sinus beats during 5 minute sequences of short (effective refractory period + 10 ms), long (80% of sinus rhythm cycle length), and variable CIs (random CIs generated between the short and long values). The order of sequences was chosen at random and activity was allowed to return to baseline (minimum of 10-minute recovery interval) before proceeding to the subsequent intervention. Importantly, each intervention was compared to its own baseline. In addition, neurons were functionally classified as afferent, efferent or convergent using the protocol outlined below.

## Cardiac electrophysiological mapping

Epicardial activation recovery intervals (ARIs), a surrogate for action potential duration, were derived from unipolar electrograms recorded from a 56-electrode sock array placed over the ventricles (Prucka CardioLab, GE Healthcare) (Figure 1A). ARIs were calculated using a customized software ScalDyn (University of Utah, Salt Lake City, UT, USA) as previously described.<sup>16, 17</sup> Global dispersion of repolarization (DOR) was calculated as the variance across all electrodes. ARIs and DORs were analyzed for the PVC and PAC beat delivered in the last minute, as well as the sinus beats following them (postextrasystolic sinus beat (PES-SB)) that were compared with baseline sinus beats (SBs) (average of 5 SBs before introduction of each extrasystolic subtype). To compare fixed with variable CI (short versus short and long versus long), at least one extrasystolic beat with a CI equal to the short as well as the long CI subtypes was induced in the last minute of variable CI sequences. Thus, the electrophysiological impact of fixed versus variable CI type was not influenced by the immediate extrasystolic CI.

### **Intrinsic cardiac neuronal recording**

A 16-channel linear microelectrode array was used to record *in vivo* extracellular activity of cardiac neurons in the ventral interventricular ganglionated plexus (VIV GP), located at the origin of the left anterior descending coronary artery below the left atrial appendage, as previously described (Figure 1A & C).<sup>13, 14</sup>

### **Functional characterization of intrinsic cardiac neurons**

Cardiac neurons were functionally classified as afferent, efferent or convergent based on their responses to cardiovascular stimuli as previously described (Figure 1F & G).<sup>13, 14</sup> Afferent neurons were defined as those that received only mechanosensory inputs by epicardial mechanical stimuli, and/or transduced changes in preload or afterload by transient occlusion of the inferior vena cava and descending thoracic aorta, respectively. Efferent neurons were defined as those that received only sympathetic and/or parasympathetic efferent inputs by bilateral stellate ganglia and cervical vagus nerve stimulation, respectively. Autonomic nerve stimulations were performed at low levels to assess direct inputs to the ICNS independent of changes in hemodynamic indices (Table S1). Neurons responding to both afferent and efferent stimuli were defined as convergent.<sup>13, 14</sup>

A significant increase or decrease ( $P < 0.05$ ) in neuronal firing frequency during the intervention compared to baseline was considered as a response to that intervention (Figure 1F & G).<sup>13, 14</sup> Cardiac phase analysis (Figure 1E) and conditional probability analysis to assess ICNS network function was performed as previously described.<sup>13, 14</sup>

### **Premature ventricular and atrial contraction delivery**

A cardiac stimulator (EPS320, MicroPace, Canterbury, AU) was used to induce PVCs and PACs from the right ventricular outflow tract (RVOT) and right atrium, respectively, using a quadripolar pacing catheter (St. Jude, St. Paul, MN, USA). Atrial and ventricular pacing thresholds were measured, and PACs and PVCs were induced using the same current (1.2 times RVOT threshold; 2 ms pulse width). In addition to PACs and PVCs, straight pacing was also performed at the same sites for 30 seconds, just overdriving the sinus rhythm cycle length ( $-20$  ms). This was performed as a control to differentiate the effects of PVC from electrical stimuli and activation from the same site.

### **Statistics**

Data are presented as mean  $\pm$  standard error of the mean. The significance level of changes in firing rate of each cardiac neuron between baseline versus stimulus interval was assessed using a statistical test developed for cortical neurons based on the Skellam distribution.<sup>18</sup> This test has been previously validated for the study of cardiac neurons.<sup>13, 14</sup> A chi-square test was used to compare the neuronal response between the different stimuli. A Wilcoxon rank-sum test or paired t-test was used as appropriate to compare hemodynamic, ARI, and heart rate variability between baseline and each intervention. Pearson correlation was used to assess the strength of the relationship between local CI and repolarization time changes. A  $p < 0.05$  was considered to be statistically significant.

## Results

### Functional characterization of intrinsic cardiac neurons

The *in vivo* activity of cardiac neurons from the VIV GP was obtained at baseline and in response to cardiovascular stimuli including PVCs and PACs. In 8 animals, the activity of 92 neurons (average:  $11.5 \pm 2.6$ ) was recorded. The basal firing frequency of the neurons was  $0.11 \pm 0.02$  Hz. Overall, based on their response to the cardiovascular stimuli, 44.6% of neurons were classified as afferent, 5.4% as efferent, and 23.9% as convergent (26.1% did not respond). A majority of neurons (92.8%) displayed activity clustered during a specific phase of the cardiac cycle, with 49.4% during systole, 25.3% during diastole, and the remaining 18.1% during both phases.

### PVC as a stimulus for intrinsic cardiac neurons

The cardiac neuronal response to PVCs of any CI was compared to afferent and efferent cardiovascular stimuli, as well as cardiac pacing. With regards to afferent stimuli, a greater percentage of neurons were impacted by PVCs (66.3%) than by activation of mechanosensitive afferent inputs (39.1%), decrease in preload by inferior vena cava occlusion (32.6%), or increase in afterload by aortic occlusion (26.9%) ( $P < 0.001$ , Figure 2A). Similarly, in regards to efferent stimuli, the neuronal response to PVCs was greater than the response to either bilateral stellate ganglia (7.6%) or vagus nerve stimulation (28.3%) ( $P < 0.0001$ , Figure 2B). It is noteworthy that the vast majority of neurons that responded to afferent or efferent cardiovascular stimuli also responded to PVCs. In addition, PVCs induced a greater response from neurons when compared to straight RVOT (19.0%) and right atrial pacing (13.6%) ( $P < 0.0001$ , Figure 2C). Of all the neurons that responded to PVCs, 19.7% only responded to RVOT pacing and 14.8% did not respond to any other cardiovascular stimuli including pacing. Therefore, neither hemodynamic changes (Table S1) nor electrical stimulation or dyssynchrony particularly explain PVCs impact on cardiac neurons.

### Impact of PVC coupling interval on intrinsic cardiac neurons

The response of cardiac neurons to PVCs of short, long, and variable CIs was compared. Overall, 29.3% of neurons responded to short CI PVCs, 39.1% to long CI PVCs, and 43.5% to variable CI PVCs ( $P < 0.05$  for short versus variable CI) (Figure 3A). The CI did not have a differential effect on afferent or efferent neurons. Twenty seven percent of afferent neurons responded to short CI PVCs, 43.9% responded to long CI PVCs and 34.1% to variable CI PVCs (Figure 3C). Forty percent of efferent neurons responded to short CI PVCs, 40.0% responded to long CI PVCs and 60.0% to variable CI PVCs (Figure 3D). Interestingly, the CI did have a differential effect on convergent neurons. More convergent neurons responded to variable CI PVCs (72.7%) than either short (40.9%) or long CI PVCs (40.9%) ( $P < 0.05$  for variable CI PVCs versus short and long CI PVCs) (Figure 3E). Further, of the convergent neurons that responded to only one PVC CI, a vast majority (75%) responded to variable CI (Figure 3B). High neuronal responses (~30%) were seen with PACs as well. For PACs, however, all three CI protocols evoked similar effects on ICNS function, whether considered as a whole or subsetted into afferent, efferent, or convergent populations (Figure 3A).

### Impact of PVC coupling interval on ICNS processing of efferent inputs

We analyzed the subset of cardiac neurons that received sympathetic and/or parasympathetic inputs (efferent and convergent neurons) to determine whether the PVC CI had an impact on sympatho-vagal balance at the level of the ICNS. Of the neurons receiving sympathetic input, a greater percentage responded to variable CI PVCs (100.0%) than either short (42.9%) or long CI PVCs (57.1%) ( $P<0.05$  for variable CI PVCs versus short and long CI PVCs) (Figure 3F). A similar trend was observed for neurons receiving parasympathetic input. Sixty nine percent of neurons responded to variable CI, 42.3% to short CI, 38.5% to long CI PVCs ( $P<0.05$  for variable CI PVCs versus short and long CI PVCs) (Figure 3G). We also performed a spectral analysis of the heart rate variability, which showed that variable CI PVCs elicited the greatest increase in sympatho-vagal balance (LF/HF) compared to baseline ( $P<0.05$ ) (Figure 3H).

### Impact of coupling interval on electro-mechanical characteristics of PVCs and PACs

We analyzed ARI, DOR and hemodynamics during PVCs and PACs to determine whether CI had an impact on cardiac electrical and mechanical indices. There was no significant difference in CI between PVCs and PACs regarding short ( $524\pm 39$  ms and  $549\pm 37$  ms respectively) or long CI ( $749\pm 56$  ms and  $765\pm 56$  ms respectively).

Mean global ARIs of short CI PVCs ( $341.9\pm 22.2$  ms) and PACs ( $347.5\pm 23.7$  ms) were shorter than long CI PVCs ( $377.6\pm 21.2$  ms) and PACs ( $389.2\pm 19.4$  ms) ( $P<0.05$  for short CI PVCs and PACs versus long CI PVCs and PACs). There was no significant difference between PVCs and PACs with short CI, and a small borderline difference between PVCs and PACs with long CI ( $P=0.05$ ). Thus, the mean global ARI seemed to be more closely related to the CI than the origin of the extrasystolic beat (Figure 4A).

The DOR (repolarization time variance), however, was greater in PVC beats ( $871\pm 148$  ms<sup>2</sup> and  $942\pm 130$  ms<sup>2</sup> for short and long CI, respectively) compared to PAC beats ( $550\pm 49$  ms<sup>2</sup> and  $498\pm 69$  ms<sup>2</sup> for short and long CI, respectively;  $P<0.05$  for PVC versus PAC). The CI did not significantly affect DOR in PVC or PAC beats, and thus, changes in DOR are likely explained by the activation sequence (Figure 4B).

Similarly, mean activation time and activation time dispersion, estimating duration and variability in ventricular activation, differed significantly between PVC and PAC beats of short and long CI ( $P<0.05$ ), whereas CI had a minimal effect on activation time of the same extrasystolic origin. Consistent with this, the extra-systolic QRS width did not differ between short and long CI PVCs ( $143\pm 4$  ms and  $141\pm 4$  ms) or PACs ( $83\pm 3$  ms and  $80\pm 3$  ms). There was no significant difference in any of these parameters between fixed and variable PVCs having the same CI (e.g., fixed short versus variable short).

Regarding hemodynamic indices (LV end systolic pressure, LV +dP/dt and -dP/dt) (Table 1) of extrasystolic beats, short CI PVCs had significantly lower values as compared to long CI PVCs ( $P<0.05$  for all) while only the LV +dP/dt differed between long and short CI PACs ( $P<0.05$ ). Therefore, both the CI and the extrasystolic origin seemed to affect hemodynamic indices, with CI being the predominant factor.



### Impact of extrasystolic coupling interval on the postextrasystolic sinus beat indices

To assess the impact of extrasystolic beats on cardiac electrical stability, ARI and DOR were analyzed for the 5 SB following extrasystolic beats (PVC and PAC) of each CI type and were compared to baseline SB before their introduction. Maximal changes in ARI were always seen on the PES-SB, returning progressively to baseline over the subsequent SBs. Maximal increase in DOR could be seen from the PES-SB to the following four SBs, since recovery toward baseline ARI values was sometime heterogeneous across different heart regions. However, overall, the mean maximal increase in DOR was also seen on the PES-SB and all comparisons were performed on this specific beat (Figure 4C & D). Overall, PVCs induced a greater increase in the PES-SB DOR than PACs ( $P<0.05$ ). A short CI also had a greater impact than long CI ES beat ( $P<0.05$ ) and finally there was a trend for an increase in DOR with variable CI as compared to fixed CI ( $P=0.10$ , paired for the exact same CI), which was driven by differences induced by PVCs ( $P=0.06$ ), but not PACs ( $P=0.8$ ). Finally, when impact of each extrasystolic subtype on PES-SB DOR was compared to its own baseline SB DOR, only the variable short CI PVCs, cumulating all aforementioned characteristics, reached statistical significance ( $P<0.05$ ).

Regarding the impact of extrasystolic beats on the PES-SB hemodynamics (Table 1), a PES potentiation was observed with an inverse relationship to the CI. The most affected index was LV +dP/dt which was significantly greater after a short than a long CI PVC ( $P<0.001$ ) or PAC ( $P<0.05$ ). Of note, the PES pause was greater after a short than a long CI PVC ( $1208\pm 97$  ms versus  $992\pm 81$  ms;  $P<0.05$ ). As a result of these compensatory effects between extrasystolic beats and PES-SB, no global heart rate or hemodynamic changes were seen during the 5 minutes of PVCs or PACs at any CI when compared to baseline (Table S1).

### “Local coupling interval” impact on extrasystolic and postextrasystolic sinus beat dispersion

We further investigated whether some electrophysiological characteristics of PVCs and PACs could explain why at similar CIs (short) PACs and PVCs (and PES-SB) display similar mean global ARI, while they have a dramatically different effect on DOR. The activation sequence when a PVC depolarizes the heart is radically differently than the SB activation sequence. Indeed, regions activated late during sinus rhythm but early during RVOT PVCs (e.g., RVOT) have a shorter CI than regions activated early during sinus rhythm but late during PVCs (e.g., apex) (Figure 5). Regional differences (up to 127 ms) in “local CI” were observed between different electrodes with RVOT PVCs. We found that electrodes with shorter local CI during PVCs displayed greater shortening in the local PVC repolarization time than electrodes with a longer local CI ( $r=0.83\pm 0.07$ ,  $P<0.001$ ). Interestingly, this local CI impact partially remained on the subsequent beat (PES-SB) with a greater shortening in repolarization in regions previously affected with a shorter local PVC CI ( $r=0.32\pm 0.05$ ,  $P<0.05$ ). On the other hand, because this “local CI effect” does not exist with PACs, they produce homogeneous changes in repolarization across the heart.

## Discussion

### Main findings

This is the first study assessing the impact of PVCs, induced at different CIs, on cardiac neuronal and electrical stability with concurrent *in vivo* cardio-neural mapping. Our main findings are:

- PVCs (even a modest burden of 10%) are a powerful stressor, altering the activity of critical cardiac neuronal populations.
- The association of an abnormal timing (CI) and activation sequence characterizing PVCs triggered these changes, with the CI being the predominant factor.
- Variable CI PVCs compared to those with fixed short or long CIs had a significantly greater impact on cardiac neurons, more specifically on convergent neurons, which are responsible for reflex processing at the level of the heart.
- Variable CI PVCs also differentially affected a greater percentage of neurons receiving sympathetic and parasympathetic input than the fixed CI PVCs. These sympathetic/parasympathetic interactions, mediated within the ICNS, may contribute to the increase in LF/HF ratio following variable CI PVCs.
- Mirroring IC neuronal changes, the greatest cardiac electrical instability in the PES-SB (i.e. increase in dispersion) was seen following variable (short) CI PVCs. Factors increasing PES-SB dispersion were: PVCs as opposed to PACs (heterogeneity in local CI across the heart), a shorter CI, and a variable CI.

### PVCs as a unique and powerful stressor: mechanistic implications

RVOT PVCs affected a large proportion (66.3%) of neurons contained within the VIV GP. These neurons are primarily associated with control of ventricular function.<sup>14</sup> Most neurons that responded to afferent and efferent cardiovascular stimuli also responded to PVCs, suggesting that PVCs preferentially engage convergent neurons (Figure 2). Similar to a previous study, 26% of neurons did not respond to afferent and efferent cardiovascular stressors used for classification of cardiac neurons.<sup>14</sup> Interestingly, however, almost half of these neurons (46%) responded to PVCs, which indicates that PVCs pose a strong and unique stress to ICNS neurons. We also analyzed the concomitant responses of this specific subset of neurons to PACs and straight pacing from the RVOT. These data indicated that the mechanism involved in triggering the changes in neuronal activity was predominately related to timing (i.e. neurons were also activated by PACs) and only a small percentage of neurons also responded to the same abnormal myocardial activation sequence (i.e. RVOT pacing). The remaining neurons responded to either a combination of timing with activation abnormalities, or involved another mechanism (i.e. concomitant activation by both PACs and RVOT pacing or neither).

Interestingly, ventricular dyssynchrony, which involves a combination of abnormal timing and activation sequence, can be measured using strain indices<sup>8</sup> and is likely to be a trigger that impacts neuronal activity. Hamdan et al. have shown that bi-ventricular pacing was



associated with lower muscle sympathetic nerve activity than right ventricular pacing alone.<sup>19</sup> Similarly, muscle sympathetic nerve activity and coronary-sinus catecholamine levels are correlated with the burden of PVCs (induced by pacing) in patients, highlighting a sympathetic neuro-humoral impact potentially involving the heart.<sup>20</sup> These changes on muscle sympathetic nerve activity were subsequently confirmed in heart failure patients during spontaneous PVCs, providing further support for the validity of our experimental model involving pacing-induced PVCs.<sup>10</sup>

A recent study provided important insight on PVC-induced dyssynchrony, showing that the timing (i.e. CI) had the greatest impact, consistent with our data.<sup>8</sup> Importantly, they reported that longer CI resulted in more pronounced LV dyssynchrony. It is interesting to note that long CI PVCs tended to affect more neurons and particularly, more afferent neurons than short CI PVCs in our study. However, our electrical data showed that PVC activation time dispersion and DOR did not differ between short and long CI and our hemodynamic data showed that short CI had a greater impact on both PVC beat and PES-SB compared to long CI. Therefore, adverse effect of PVCs is not solely hemodynamically mediated (Tables 1 & S1). Rather, a greater preload (with longer CI PVCs), although inducing a better overall hemodynamic profile, may exaggerate mechanical stretch on the myocardial wall, thereby increasing activity in sensory neurites that are locally present.<sup>12, 21</sup>

Finally, perturbations in atrio-ventricular relationship are known to increase muscle sympathetic nerve activity,<sup>22</sup> especially during closely coupled atrial and ventricular systole.<sup>23</sup> We observed similar features (close systolic coupling) during long CI PVCs, which could have had an additional impact on ICNS neurons.

### **Impact of variable coupling PVCs on ICNS network function**

Our data demonstrates that variable CI PVCs had a significantly greater impact on cardiac neurons, especially on convergent neurons, the local reflex processors. We compared the functional connectivity of neurons that responded to variable CI PVCs versus those that did not. Interestingly, we observed functional network connectivity was greater with neurons that responded to variable CI PVCs (Figure 6). Variable CI PVCs seem to have a more complex impact on cardiac neurons than just the addition of short and long CI PVCs. Indeed, we have shown that most (75%) convergent neurons affected by one CI PVC type were only activated by variable CI PVCs (Figure 3B). Similarly, variable CI PVCs differentially affected a greater percentage of neurons receiving sympathetic/parasympathetic inputs (Figure 3F & G). Finally, there was no difference in the percentage of afferent neurons affected (Figure 3C). Therefore, unpredictability in CI appeared to be a specific trigger that a subpopulation of convergent neurons can detect, further causing sympatho-vagal imbalance. This cardio-cardiac reflex, likely also involving higher centers in the neuraxis (Figure 7), may subsequently impact cardiomyocyte function and lead to electrical instability.

Enhanced response of neurons to a variable compared to constant stimulus has been reported in sensory neurons in visual, auditory, and olfactory system, a concept known as neural adaptation.<sup>24, 25</sup> Similarly, in the cardiovascular system, it has been previously shown that sympathetic nerve activity measured by muscle sympathetic nerve activity was greater when

the heart was paced irregularly, and these findings were independent of hemodynamic changes.<sup>26</sup> We speculate that variability of PVC CI compared to fixed CI may prevent neural adaptation and play an important role in reflex activation of the ANS.

### **Impact of PVCs on cardiac electrical stability: PES-SB dispersion of repolarization**

Increase in the SB DOR has been described as arrhythmogenic, being a requirement for electrical reentry and lethal ventricular arrhythmias.<sup>27, 28</sup> Furthermore, DOR has been strongly correlated with the Tpeak-Tend interval, which is a predictor of sudden cardiac death risk in most CMPs as well as in more heterogeneous populations.<sup>29</sup> Similarly, other electrocardiogram parameters estimating the spatial or temporal<sup>30-32</sup> DOR have been shown to improve sudden cardiac death prediction.

More specifically, a short-long sequence has been described as a major trigger for ventricular arrhythmias.<sup>33</sup> Therefore, part of the arrhythmogenesis may be explained by the PES-SB DOR<sup>34</sup> (after the short CI PVC) and another by the CI of the subsequent PVC. PES-SB dispersion was globally higher following PVC (versus same CI PAC) because of their non-uniform local CI across the heart. A malignant short-long-short sequence following a PAC (as first short) has never been reported. Heart regions that depolarize late during sinus rhythm and early during PVCs (shorter local CI) are more impacted (shorter repolarization) than regions having a longer local CI (Figure 5). Interestingly, PVCs arising from very late activated regions in sinus rhythm (e.g. aortic cusps, epicardial) are associated with worse outcomes.<sup>4, 5, 7</sup> Finally, variable CI PVCs increased PES-SB dispersion as compared to fixed CI PVCs, despite comparisons following similar CI. Therefore, impact of variable CI on neuronal stability was the last potential mechanistic component of the increase in PES-SB dispersion that we could identify in the present study. Indeed, sympathetic stimulation has been shown to increase DOR experimentally in porcine models<sup>17, 35</sup> as well as in humans<sup>16</sup> and lead to lethal ventricular arrhythmias.<sup>11</sup> By carrying all deleterious characteristics, only variable short CI PVC induced a statistically significant increase in the PES-SB dispersion as compared to baseline. The level of dispersion necessary to initiate ventricular arrhythmias remains unknown, and given the rare incidence of such event, additional stress-mediated autonomic involvement is likely necessary to provide sufficient functional arrhythmogenic substrate.<sup>16, 36, 37</sup> Interestingly, in addition to inducing a greater PES-SB DOR (i.e. vulnerability), a greater CI variability would also increase the likelihood for a subsequent PVC to trigger an arrhythmia if a specific CI is required. Finally, intracellular calcium handling likely involved in acute changes in DOR may translate into heterogeneous ion channel remodeling, resulting in marked heterogeneity in action potential configurations and durations, as reported in a chronic canine model of PVC-induced CMP,<sup>9</sup> which may lead to a more sustained arrhythmogenic substrate.

Neuromodulation represents an attractive approach that has been shown to specifically inhibit deleterious activity within the ICNS<sup>15, 38</sup> or intrathoracic extracardiac ganglia,<sup>39</sup> thereby mitigating the substrate and preventing arrhythmias. Further, it has anti-fibrotic properties<sup>40</sup> and myocardial fibrosis has been characterized in a model of PVC-induced CMP<sup>41</sup> and could compromise recovery, even after successful PVC suppression.

## Limitations

General anesthetics may suppress evoked responses in the ANS. However, after surgical preparation, we switched to  $\alpha$ -chloralose, which has minimal effects on ANS reflexes. Neuronal recording was selectively performed in the VIV GP (1 of 11 GPs in porcine heart).<sup>12</sup> However, GP have been described to have spatially divergent receptive fields, capable of transducing information from widespread cardiac regions, and VIV GP is primarily associated with control of ventricular function.<sup>21</sup> It is also noteworthy that there is a high degree of communication at all levels of the ANS and changes in LF/HF following PVCs, believed to reflect global sympatho-vagal balance and its effect on cardiac dynamics,<sup>42</sup> seemed to mirror the “local” impact on VIV GP neurons.

This unique set of data assessing acute changes would benefit from confirmation in a chronic PVC model, in the setting of heart disease, and prompt further assessment of functional and anatomopathological remodeling at different levels of the neuraxis. Additionally, whether the differential effect of the CI seen on cardiac electrical stability and neuronal behavior is dependent on a specific burden<sup>43</sup> or a PVC location remain unknown. Indeed, we studied PVCs from only one location (RVOT), which is the most commonly encountered clinically, and investigating different locations in this set of animals was not feasible. A 10% burden induced acutely was enough to have a significant impact, which has been previously described as the lowest burden inducing a reversible CMP,<sup>44</sup> particularly with an epicardial origin.<sup>7</sup> Although our data suggested that part of destabilizing cardiac repolarization changes were mediated through PVC-induced changes in IC neural activity, our study was not sufficiently powered to establish a direct temporal link between these 2 components.

Surrogate markers of arrhythmogenesis have been used in this study rather than inducibility testing, which would have compromised our model of PVC delivery subsequent to sensed SB. Moreover, cardioversion shocks required to resuscitate animals from a ventricular arrhythmia would have disrupted and/or dislodged our neuronal recording interface. An extensive literature has correlated these surrogates with sudden cardiac death.<sup>27–32</sup>

## Supplementary Material

Refer to Web version on PubMed Central for supplementary material.

## Acknowledgments

**Sources of Funding:** This work was supported by National Institutes of Health (NIH) National Heart, Lung, and Blood Institute (NHLBI) Grant 4R01HL084261-09 to K.S., NIH Stimulating Peripheral Activity to Relieve Conditions (SPARC) Grant 1OT2OD023848-01 to K.S., and NIH SPARC Grant 5U18EB021799-02 to J.L.A. D.H. was supported by a Federation Francaise de Cardiology Grant. P.S.R. was supported by NIH NHLBI Grant 5F31HL127974-02.

## References

1. Yarlagadda RK, Iwai S, Stein KM, Markowitz SM, Shah BK, Cheung JW, Tan V, Lerman BB, Mittal S. Reversal of cardiomyopathy in patients with repetitive monomorphic ventricular ectopy originating from the right ventricular outflow tract. *Circulation*. 2005; 112:1092–1097. [PubMed: 16103234]

2. Leenhardt A, Glaser E, Burguera M, Nurnberg M, Maison-Blanche P, Coumel P. Short-coupled variant of torsade de pointes. A new electrocardiographic entity in the spectrum of idiopathic ventricular tachyarrhythmias. *Circulation*. 1994; 89:206–215. [PubMed: 8281648]
3. Viskin S, Rosso R, Rogowski O, Belhassen B. The “short-coupled” variant of right ventricular outflow ventricular tachycardia: a not-so-benign form of benign ventricular tachycardia? *J Cardiovasc Electrophysiol*. 2005; 16:912–916. [PubMed: 16101636]
4. Kawamura M, Badhwar N, Vedantham V, Tseng ZH, Lee BK, Lee RJ, Marcus GM, Olgin JE, Gerstenfeld EP, Scheinman MM. Coupling interval dispersion and body mass index are independent predictors of idiopathic premature ventricular complex-induced cardiomyopathy. *J Cardiovasc Electrophysiol*. 2014; 25:756–762. [PubMed: 24612052]
5. Bradfield JS, Homsí M, Shivkumar K, Miller JM. Coupling interval variability differentiates ventricular ectopic complexes arising in the aortic sinus of valsalva and great cardiac vein from other sources: mechanistic and arrhythmic risk implications. *J Am Coll Cardiol*. 2014; 63:2151–2158. [PubMed: 24657687]
6. Lee CH, Park KH, Nam JH, Lee J, Choi YJ, Kong EJ, Lee HW, Son JW, Kim U, Park JS, Kim YJ, Shin DG. Increased variability of the coupling interval of premature ventricular contractions as a predictor of cardiac mortality in patients with left ventricular dysfunction. *Circ J*. 2015; 79:2360–2366. [PubMed: 26356836]
7. Hamon D, Sadron M, Bradfield JS, Chaachoui N, Tung R, Elayi C, Vaseghi M, Dhanjal TS, Boyle NG, Maury P, Shivkumar K, Lellouche N. A New Combined Parameter to Predict Premature Ventricular Complexes Induced Cardiomyopathy: Impact and Recognition of Epicardial Origin. *J Cardiovasc Electrophysiol*. 2016; 27:709–17. [PubMed: 26924618]
8. Potfay J, Kaszala K, Tan AY, Sima AP, Gorcsan J 3rd, Ellenbogen KA, Huizar JF. Abnormal Left Ventricular Mechanics of Ventricular Ectopic Beats: Insights Into Origin and Coupling Interval in Premature Ventricular Contraction-Induced Cardiomyopathy. *Circ Arrhythm Electrophysiol*. 2015; 8:1194–1200. [PubMed: 26297787]
9. Wang Y, Eltit JM, Kaszala K, Tan A, Jiang M, Zhang M, Tseng GN, Huizar JF. Cellular mechanism of premature ventricular contraction-induced cardiomyopathy. *Heart Rhythm*. 2014; 11:2064–2072. [PubMed: 25046857]
10. Maslov PZ, Breskovic T, Brewer DN, Shoemaker JK, Dujic Z. Recruitment pattern of sympathetic muscle neurons during premature ventricular contractions in heart failure patients and controls. *Am J Physiol Regul Integr Comp Physiol*. 2012; 303:R1157–1164. [PubMed: 23054172]
11. Fukuda K, Kanazawa H, Aizawa Y, Ardell JL, Shivkumar K. Cardiac innervation and sudden cardiac death. *Circ Res*. 2015; 116:2005–2019. [PubMed: 26044253]
12. Armour JA. Potential clinical relevance of the ‘little brain’ on the mammalian heart. *Exp Physiol*. 2008; 93:165–176. [PubMed: 17981929]
13. Beaumont E, Salavatian S, Southerland EM, Vinet A, Jacquemet V, Armour JA, Ardell JL. Network interactions within the canine intrinsic cardiac nervous system: implications for reflex control of regional cardiac function. *J Physiol*. 2013; 591:4515–4533. [PubMed: 23818689]
14. Rajendran PS, Nakamura K, Ajijola OA, Vaseghi M, Armour JA, Ardell JL, Shivkumar K. Myocardial infarction induces structural and functional remodelling of the intrinsic cardiac nervous system. *J Physiol*. 2016; 594:321–341. [PubMed: 26572244]
15. Gibbons DD, Southerland EM, Hoover DB, Beaumont E, Armour JA, Ardell JL. Neuromodulation targets intrinsic cardiac neurons to attenuate neuronally mediated atrial arrhythmias. *Am J Physiol Regul Integr Comp Physiol*. 2012; 302:R357–364. [PubMed: 22088304]
16. Vaseghi M, Lux RL, Mahajan A, Shivkumar K. Sympathetic stimulation increases dispersion of repolarization in humans with myocardial infarction. *Am J Physiol Heart Circ Physiol*. 2012; 302:H1838–1846. [PubMed: 22345568]
17. Vaseghi M, Zhou W, Shi J, Ajijola OA, Hadaya J, Shivkumar K, Mahajan A. Sympathetic innervation of the anterior left ventricular wall by the right and left stellate ganglia. *Heart Rhythm*. 2012; 9:1303–1309. [PubMed: 22465457]
18. Shin HC, Aggarwal V, Acharya S, Schieber MH, Thakor NV. Neural decoding of finger movements using Skellam-based maximum-likelihood decoding. *IEEE Trans Biomed Eng*. 2010; 57:754–760. [PubMed: 19403361]

19. Hamdan MH, Zagrodzky JD, Joglar JA, Sheehan CJ, Ramaswamy K, Erdner JF, Page RL, Smith ML. Biventricular pacing decreases sympathetic activity compared with right ventricular pacing in patients with depressed ejection fraction. *Circulation*. 2000; 102:1027–1032. [PubMed: 10961968]
20. Smith ML, Hamdan MH, Wasmund SL, Kneip CF, Joglar JA, Page RL. High-frequency ventricular ectopy can increase sympathetic neural activity in humans. *Heart Rhythm*. 2010; 7:497–503. [PubMed: 20184979]
21. Cardinal R, Page P, Vermeulen M, Ardell JL, Armour JA. Spatially divergent cardiac responses to nicotinic stimulation of ganglionated plexus neurons in the canine heart. *Auton Neurosci*. 2009; 145:55–62. [PubMed: 19071069]
22. Taylor JA, Morillo CA, Eckberg DL, Ellenbogen KA. Higher sympathetic nerve activity during ventricular (VVI) than during dual-chamber (DDD) pacing. *J Am Coll Cardiol*. 1996; 28:1753–1758. [PubMed: 8962562]
23. Hamdan MH, Zagrodzky JD, Page RL, Wasmund SL, Sheehan CJ, Adamson MM, Joglar JA, Smith ML. Effect of P-wave timing during supraventricular tachycardia on the hemodynamic and sympathetic neural response. *Circulation*. 2001; 103:96–101. [PubMed: 11136692]
24. De Palo G, Facchetti G, Mazzolini M, Menini A, Torre V, Altafini C. Common dynamical features of sensory adaptation in photoreceptors and olfactory sensory neurons. *Sci Rep*. 2013; 3:1251. [PubMed: 23409242]
25. Grill-Spector K, Henson R, Martin A. Repetition and the brain: neural models of stimulus-specific effects. *Trends Cogn Sci*. 2006; 10:14–23. [PubMed: 16321563]
26. Segerson NM, Sharma N, Smith ML, Wasmund SL, Kowal RC, Abedin M, Macgregor JF, Pai RK, Freedman RA, Klein RC, Wall TS, Stoddard G, Hamdan MH. The effects of rate and irregularity on sympathetic nerve activity in human subjects. *Heart Rhythm*. 2007; 4:20–26. [PubMed: 17198984]
27. Kuo CS, Munakata K, Reddy CP, Surawicz B. Characteristics and possible mechanism of ventricular arrhythmia dependent on the dispersion of action potential durations. *Circulation*. 1983; 67:1356–1367. [PubMed: 6851031]
28. Vassallo JA, Cassidy DM, Kindwall KE, Marchlinski FE, Josephson ME. Nonuniform recovery of excitability in the left ventricle. *Circulation*. 1988; 78:1365–1372. [PubMed: 3191591]
29. Panikath R, Reinier K, Uy-Evanado A, Teodorescu C, Hattenhauer J, Mariani R, Gunson K, Jui J, Chugh SS. Prolonged Tpeak-to-tend interval on the resting ECG is associated with increased risk of sudden cardiac death. *Circ Arrhythm Electrophysiol*. 2011; 4:441–447. [PubMed: 21593198]
30. Ichikawa T, Sobue Y, Kasai A, Kiyono K, Hayano J, Yamamoto M, Okuda K, Watanabe E, Ozaki Y. Beat-to-beat T-wave amplitude variability in the risk stratification of right ventricular outflow tract-premature ventricular complex patients. *Europace*. 2016; 18:138–145. [PubMed: 25733552]
31. Swerdlow C, Chow T, Das M, Gillis AM, Zhou X, Abeyratne A, Ghanem RN. Intracardiac electrogram T-wave alternans/variability increases before spontaneous ventricular tachyarrhythmias in implantable cardioverter-defibrillator patients: a prospective, multi-center study. *Circulation*. 2011; 123:1052–1060. [PubMed: 21357826]
32. Verrier RL, Klingenhoben T, Malik M, El-Sherif N, Exner DV, Hohnloser SH, Ikeda T, Martinez JP, Narayan SM, Nieminen T, Rosenbaum DS. Microvolt T-wave alternans physiological basis, methods of measurement, and clinical utility--consensus guideline by International Society for Holter and Noninvasive Electrocardiology. *J Am Coll Cardiol*. 2011; 58:1309–1324. [PubMed: 21920259]
33. Gomes JA, Alexopoulos D, Winters SL, Deshmukh P, Fuster V, Suh K. The role of silent ischemia, the arrhythmic substrate and the short-long sequence in the genesis of sudden cardiac death. *J Am Coll Cardiol*. 1989; 14:1618–1625. [PubMed: 2584549]
34. Viskin S, Heller K, Barron HV, Kitzis I, Hamdan M, Olgin JE, Wong MJ, Grant SE, Lesh MD. Postextrasystolic U wave augmentation, a new marker of increased arrhythmic risk in patients without the long QT syndrome. *J Am Coll Cardiol*. 1996; 28:1746–1752. [PubMed: 8962561]
35. Yagishita D, Chui RW, Yamakawa K, Rajendran PS, Ajjola OA, Nakamura K, So EL, Mahajan A, Shivkumar K, Vaseghi M. Sympathetic nerve stimulation, not circulating norepinephrine, modulates T-peak to T-end interval by increasing global dispersion of repolarization. *Circ Arrhythm Electrophysiol*. 2015; 8:174–185. [PubMed: 25532528]

36. Han J, Moe GK. Nonuniform Recovery of Excitability in Ventricular Muscle. *Circ Res.* 1964; 14:44–60. [PubMed: 14104163]
37. Vaseghi M, Shivkumar K. The role of the autonomic nervous system in sudden cardiac death. *Prog Cardiovasc Dis.* 2008; 50:404–419. [PubMed: 18474284]
38. Yu L, Scherlag BJ, Li S, Sheng X, Lu Z, Nakagawa H, Zhang Y, Jackman WM, Lazzara R, Jiang H, Po SS. Low-level vagosympathetic nerve stimulation inhibits atrial fibrillation inducibility: direct evidence by neural recordings from intrinsic cardiac ganglia. *J Cardiovasc Electrophysiol.* 2010; 22:455–463. [PubMed: 20946225]
39. Shen MJ, Shinohara T, Park HW, Frick K, Ice DS, Choi EK, Han S, Maruyama M, Sharma R, Shen C, Fishbein MC, Chen LS, Lopshire JC, Zipes DP, Lin SF, Chen PS. Continuous low-level vagus nerve stimulation reduces stellate ganglion nerve activity and paroxysmal atrial tachyarrhythmias in ambulatory canines. *Circulation.* 2011; 123:2204–2212. [PubMed: 21555706]
40. Wang Z, Yu L, Wang S, Huang B, Liao K, Saren G, Tan T, Jiang H. Chronic intermittent low-level transcutaneous electrical stimulation of auricular branch of vagus nerve improves left ventricular remodeling in conscious dogs with healed myocardial infarction. *Circ Heart Fail.* 2014; 7:1014–1021. [PubMed: 25332149]
41. Tanaka Y, Rahmutula D, Duggirala S, Nazer B, Fang Q, Olgin J, Sievers R, Gerstenfeld EP. Diffuse fibrosis leads to a decrease in unipolar voltage: Validation in a swine model of premature ventricular contraction-induced cardiomyopathy. *Heart Rhythm.* 2016; 13:547–554. [PubMed: 26416621]
42. Piccirillo G, Ogawa M, Song J, Chong VJ, Joung B, Han S, Magri D, Chen LS, Lin SF, Chen PS. Power spectral analysis of heart rate variability and autonomic nervous system activity measured directly in healthy dogs and dogs with tachycardia-induced heart failure. *Heart Rhythm.* 2009; 6:546–552. [PubMed: 19324318]
43. Tan AY, Hu YL, Potfay J, Kaszala K, Howren M, Sima AP, Shultz M, Koneru JN, Ellenbogen KA, Huizar JF. Impact of ventricular ectopic burden in a premature ventricular contraction-induced cardiomyopathy animal model. *Heart Rhythm.* 2016; 13:755–761. [PubMed: 26586453]
44. Baman TS, Lange DC, Ilg KJ, Gupta SK, Liu TY, Alguire C, Armstrong W, Good E, Chugh A, Jongnarangsin K, Pelosi F Jr, Crawford T, Ebinger M, Oral H, Morady F, Bogun F. Relationship between burden of premature ventricular complexes and left ventricular function. *Heart Rhythm.* 2010; 7:865–869. [PubMed: 20348027]



### Clinical Implications

Currently, the clinical approach for PVC patients consists of ruling out a structural arrhythmogenic substrate and thereby, classifying the PVC as “benign”. However, cardiac events are known to occur with “benign” PVCs,<sup>2, 3, 5</sup> and we have yet to decipher the mechanism behind this small, but very real risk. This study provides important mechanistic insights into mechano-electrical feedback (mediated through cardiac neurons) that have the potential to contribute to a new avenue of investigation and allow more precise risk stratification in the future. If further translational and clinical data supports these findings, temporal and spatial electrocardiogram tools focusing on PES-SB repolarization and PVC CI variability should be employed and further developed to improve risk stratification in PVC patients, and potentially prompt more aggressive prophylactic management. Finally, understanding neural signatures associated with PVC-induced CMP/arrhythmogenesis will pave the way for novel therapies targeting the ANS to prevent cardiac disease.

**WHAT IS KNOWN**

- Variability in premature ventricular contraction (PVC) coupling interval (CI) increases the risk of cardiomyopathy and sudden death, yet the underlying mechanisms remain unknown.
- The autonomic nervous system regulates cardiac electrical and mechanical indices, and its dysregulation plays an important role in cardiac disease pathogenesis. The intrinsic cardiac nervous system (ICNS), a neural network on the heart, is the first level involved in reflex control and impacted by cardiac injury.

**WHAT THE STUDY ADDS**

- PVCs are a powerful stressor for the ICNS, with the CI being the predominant factor. Activation sequence is another important mechanism for the increase in dispersion of repolarization (i.e. cardiac instability) on sinus beats following PVCs.
- PVCs with variable CI affect critical populations of ICNS neurons and alter cardiac repolarization, more than those with fixed short or long CI.
- We report, using a novel cardio-neural mapping approach, that PVC-induced neural and electrophysiological changes may be critical for arrhythmogenesis and remodeling leading to cardiomyopathy. Studies like ours, that provide a better understanding of neural control of cardiac function in healthy and disease states, will pave the way for neuroscience-based cardiovascular therapeutics.

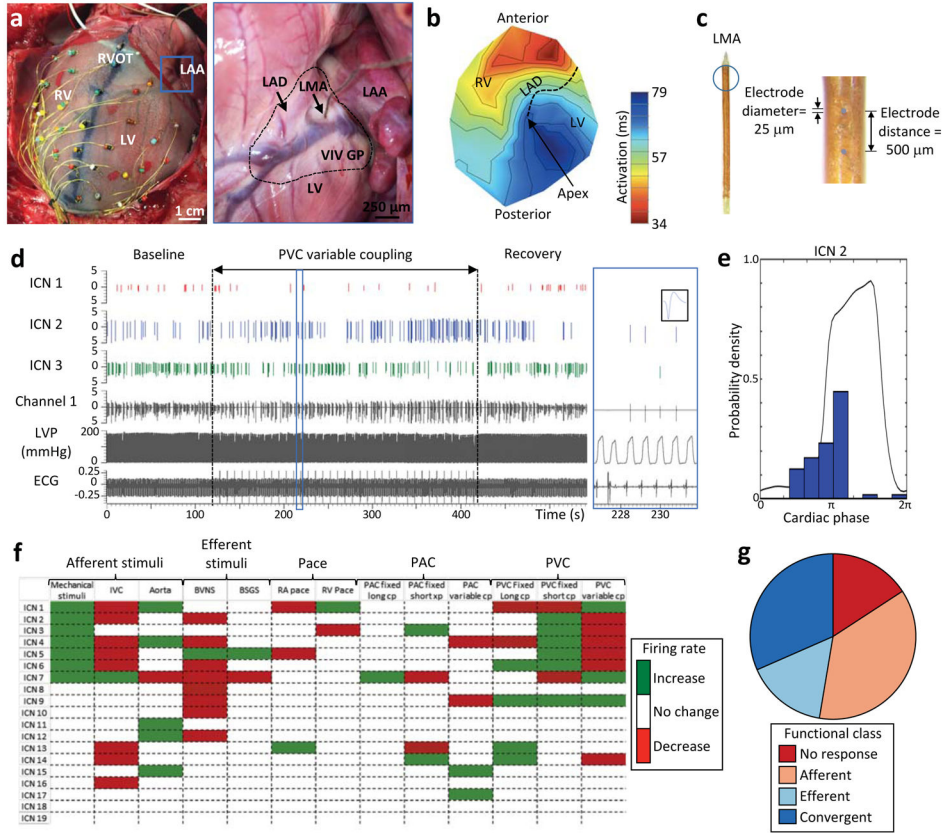


**Figure 1.** Cardiac electrophysiological mapping and neuronal recording: methods. **(A)** Porcine heart with 56-electrode sock array around ventricular epicardium to record unipolar cardiac electrograms and a linear microelectrode array (LMA) in the ventral interventricular ganglionated plexus (VIV GP) to record intrinsic cardiac neuronal activity. Premature ventricular contractions (PVCs) were induced via right ventricular outflow tract (RVOT) pacing. Blue box in left panel is a higher magnification of VIV GP (black dashed line in right panel) with embedded LMA. **(B)** Representative polar activation map of PVC induced from the RVOT. Black dotted line indicates location of left anterior descending coronary artery (LAD). **(C)** 16-channel LMA used to record neuronal activity. **(D)** Representative trace showing the activity of three intrinsic cardiac neurons (ICN 1, 2 and 3) from a single electrode (channel 1) of the LMA as well as left ventricular pressure (LVP) and electrocardiogram (ECG). Black vertical dotted lines indicate the time period in which variable coupling interval PVCs were delivered. Blue box is a higher magnification of the trace with an inset showing the waveform of ICN 2. **(E)** Basal activity of one of the neurons from panel D (ICN 2) in relation to the cardiac cycle. Note that the activity of this neuron is predominately clustered during isovolumetric contraction. **(F)** Summary of evoked changes in neuronal activity in response to PVCs as well as other cardiovascular stimuli from a single animal. Horizontal rows represent the response of an individual neuron to a given stimulus (vertical columns). Green and red indicate significant increase or decreases in activity ( $P < 0.05$ ), respectively. **(G)** Functional classification of neurons depicted in panel F. Neurons

were classified as afferent, efferent, or convergent based on their responses to the cardiovascular stimuli. Afferent neurons were defined as those that responded only to epicardial mechanical stimuli of the right (RV) or left ventricle (LV); transient occlusion of the inferior vena cava (IVC); and/or transient occlusion of the descending thoracic aorta. Efferent neurons were defined as those that responded only to electrical stimulation of the bilateral vagus nerves (BVNS) and/or stellate ganglia (BSGS). Neurons that responded to activation of both afferent and efferent inputs were defined as convergent. PAC, premature atrial contraction; RA, right atrium.

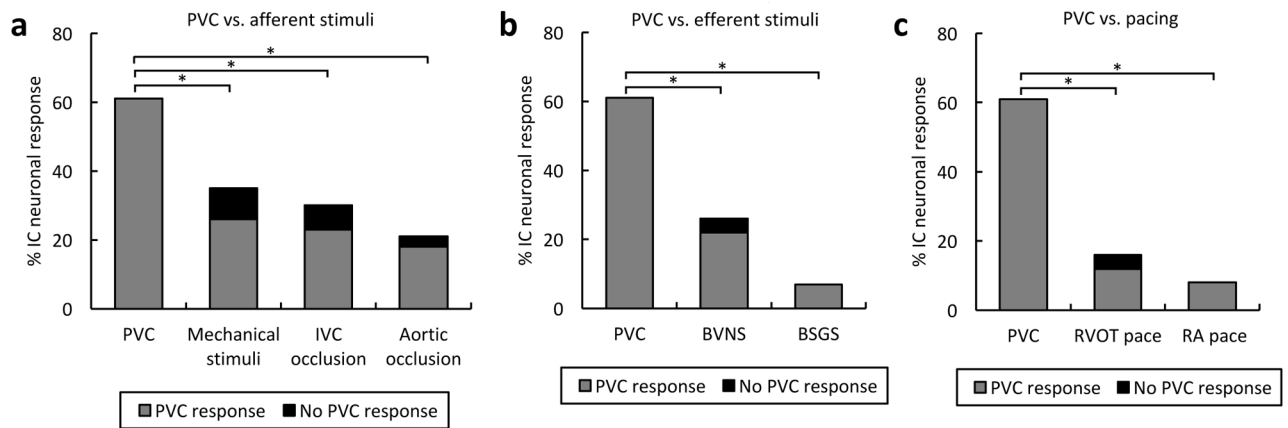


**Figure 2.**

PVCs are a powerful and unique cardiovascular stimulus. **(A)** Percentage of intrinsic cardiac (IC) neurons responding to premature ventricular contractions (PVCs) versus afferent cardiovascular stimuli. **(B)** Percentage of neurons responding to PVCs versus efferent cardiovascular stimuli. **(C)** Percentage of neurons responding to PVCs versus pacing. Note that the vast majority of neurons that responded to afferent and efferent cardiovascular stimuli, as well as pacing, also responded to PVCs. BSGS, bilateral stellate ganglia stimulation; BVNS; bilateral vagus nerve stimulation; IVC, inferior vena cava; RA, right atrium; RVOT, right ventricular outflow tract. \*,  $P < 0.001$ .

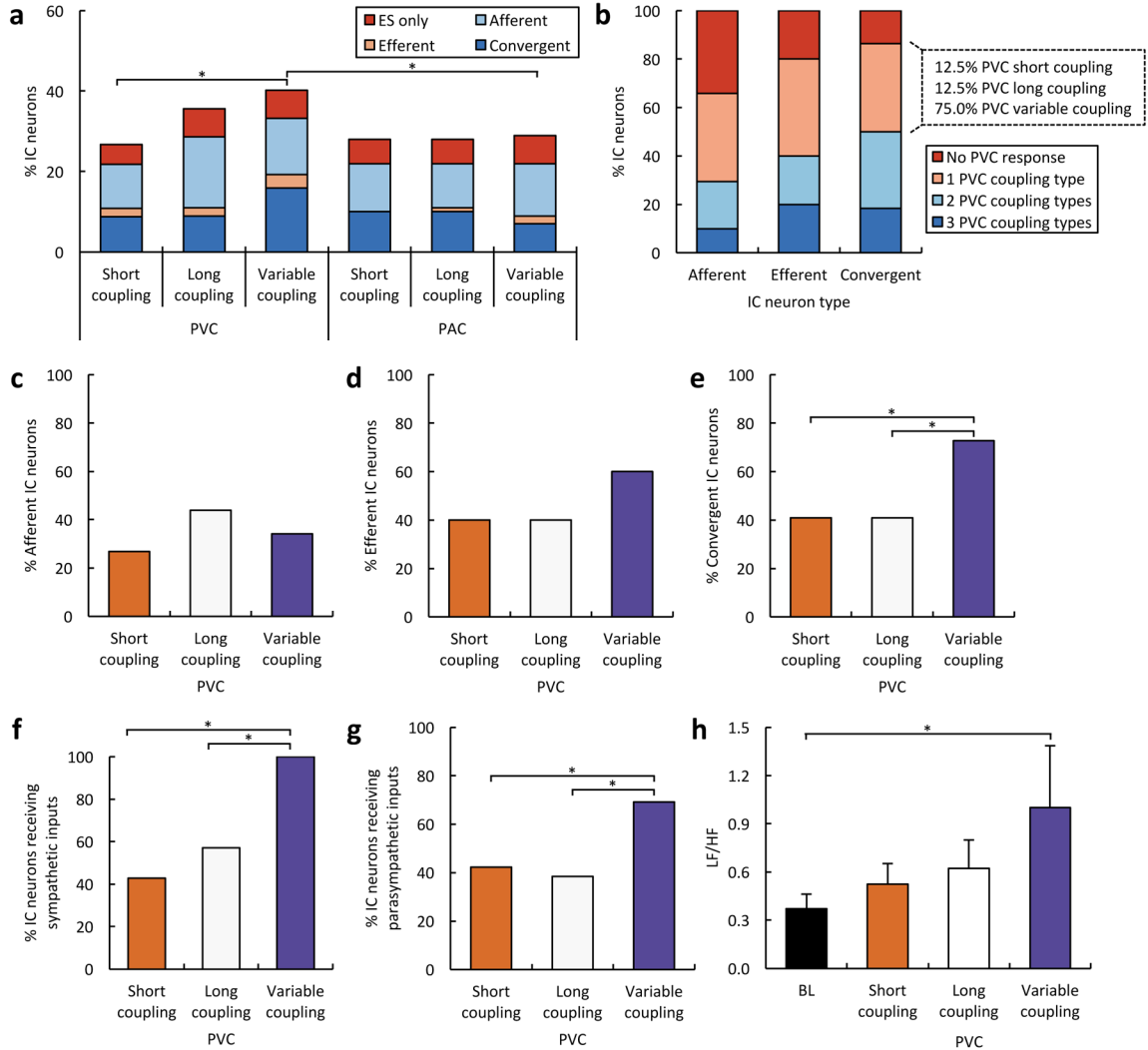


**Figure 3.** Impact of PVC coupling interval on intrinsic cardiac neurons. **(A)** Functional classification of intrinsic cardiac (IC) neurons responding to premature ventricular (PVCs) and atrial contractions (PAC) of different coupling intervals. Note that a subset of neurons responded only to the extrasystole (ES), and none of the other afferent and efferent cardiovascular stimuli. **(B)** Percentage afferent, efferent and convergent neurons that responded to multiple PVC types. Note that of convergent neurons that responded to only one PVC, the vast majority responded to variable coupling interval PVCs. **(C)** Percentage of afferent neurons responding to PVCs of different coupling intervals. **(D)** Percentage of efferent neurons responding to PVCs of different coupling intervals. **(E)** Percentage of convergent neurons responding to PVCs of different coupling intervals. **(F)** Percentage of neurons receiving sympathetic inputs from the stellate ganglia responding to PVCs of different coupling intervals. **(G)** Percentage of neurons receiving parasympathetic inputs from the vagus nerve responding to PVCs of different coupling intervals. **(H)** Low frequency (LF)/high frequency (HF) ratio following PVCs of different coupling intervals versus baseline (BL). \*,  $P < 0.05$ .



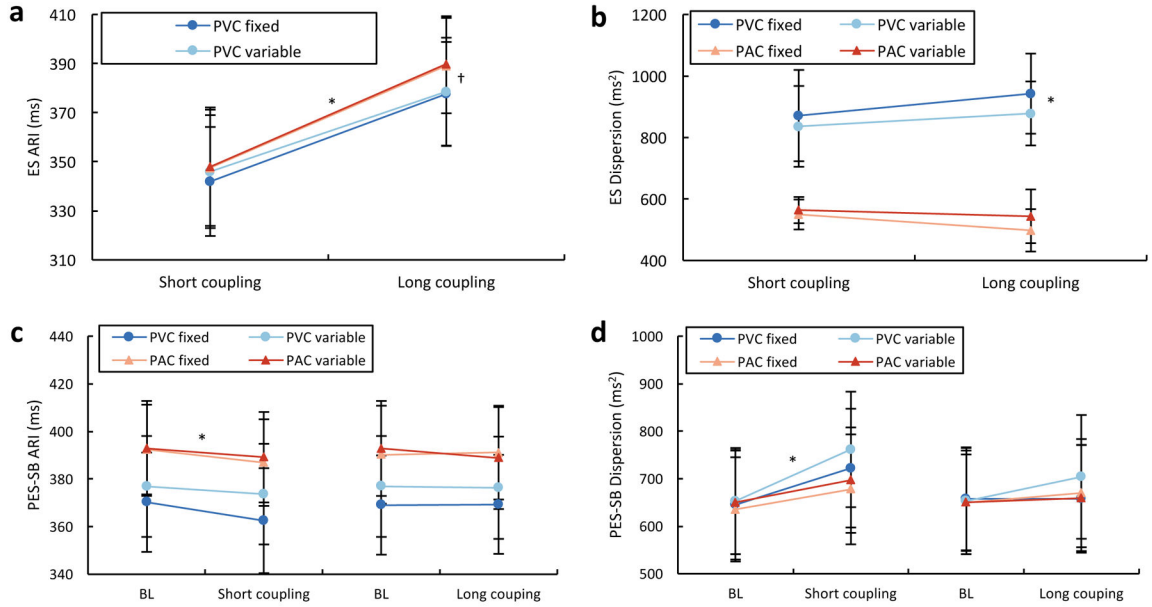


**Figure 4.**

Impact of PVCs coupling interval on cardiac electrophysiology. **(A)** Activation recovery intervals (ARIs) of ventricular and atrial extrasystolic (ES) beats of different coupling intervals. \*,  $P < 0.05$  for short versus long coupling premature ventricular (PVCs) and atrial contractions (PACs). †,  $P < 0.05$  for long coupling PVCs versus PACs. **(B)** Dispersion of repolarization of ventricular and atrial ES beats of different coupling intervals. \*,  $P < 0.05$  for short and long coupling PVCs versus PACs. **(C)** ARIs of postextrasystolic sinus beat (PES-SB) following PVCs and PACs of different coupling intervals versus baseline (BL) sinus beat. \*,  $P < 0.05$  for fixed short coupling PACs versus BL. **(D)** Dispersion of ARI for PES-SB following PVCs and PACs of different coupling intervals versus BL sinus beat. \*,  $P < 0.05$  for variable short coupling PVC versus BL.

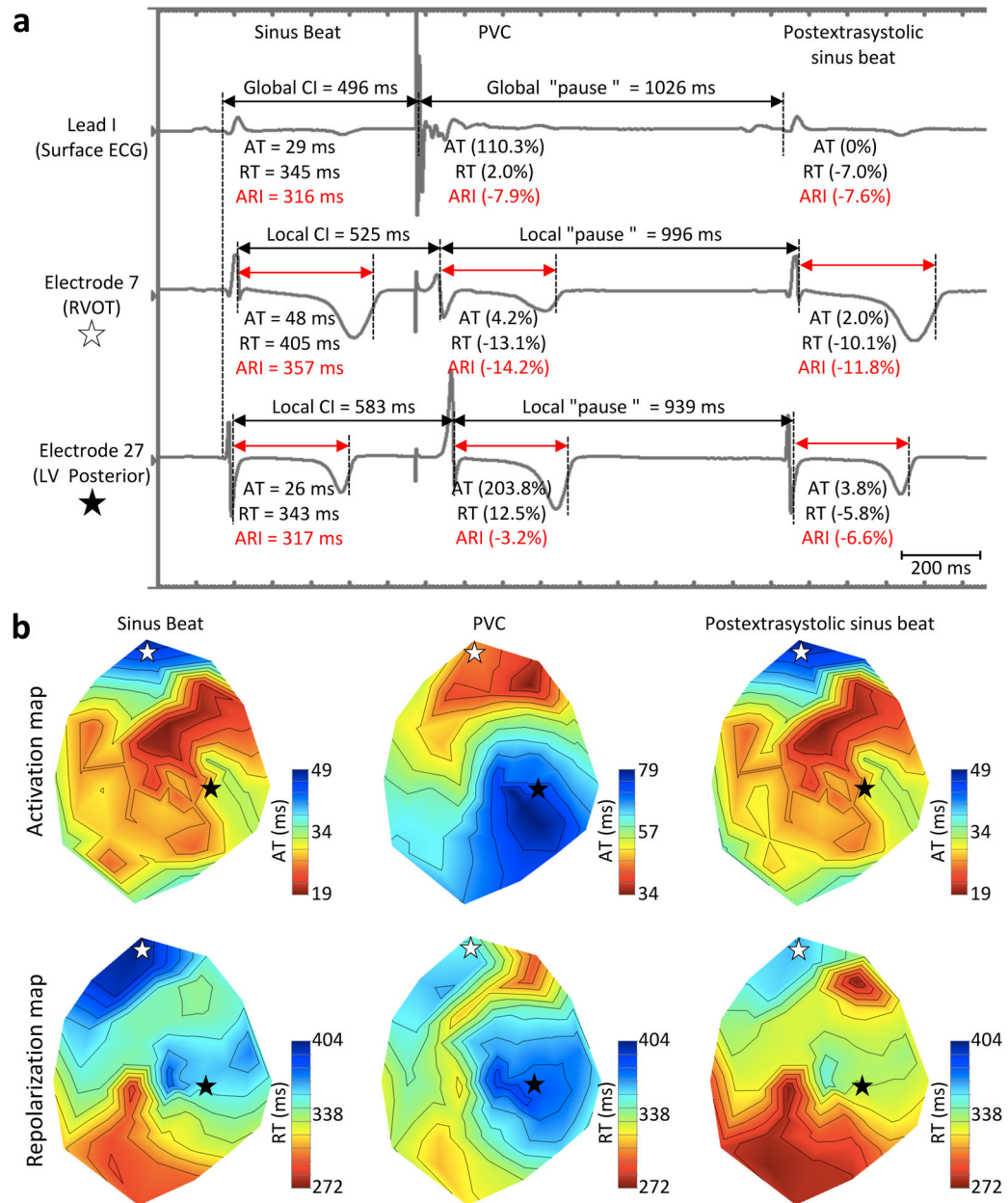


**Figure 5.**

PVC local coupling interval impact on repolarization. (A) Representative trace showing a sinus beat followed by a premature ventricular contraction (PVC) induced at a coupling of 496 ms and the subsequent postextrasystolic sinus beat on 1) surface ECG lead I, 2) a unipolar sock electrode recorded from the right ventricular outflow tract (RVOT), and 3) from the left ventricular (LV) posterior-apical wall. Overall, mean activation time (AT), repolarization time (RT) and activation recovery interval (ARI) across the heart as well as values recorded from RVOT and LV posterior electrodes are displayed under each respective trace. (B) Polar map showing myocardial activation during the sinus beat and the subsequent PVC and postextrasystolic beats. White and black stars indicate location of RVOT and LV

posterior-apical wall electrodes, respectively. Note that the RVOT electrode, which had a shorter local CI than the LV posterior-apical one, was characterized by a greater shortening in RT that remained on the postextrasystolic-sinus beat while activation pattern was back to normal. Such PVC-induced arrhythmogenic substrate may increase the likelihood for subsequent “critically-timed” PVCs to trigger re-entry mediated ventricular arrhythmias.

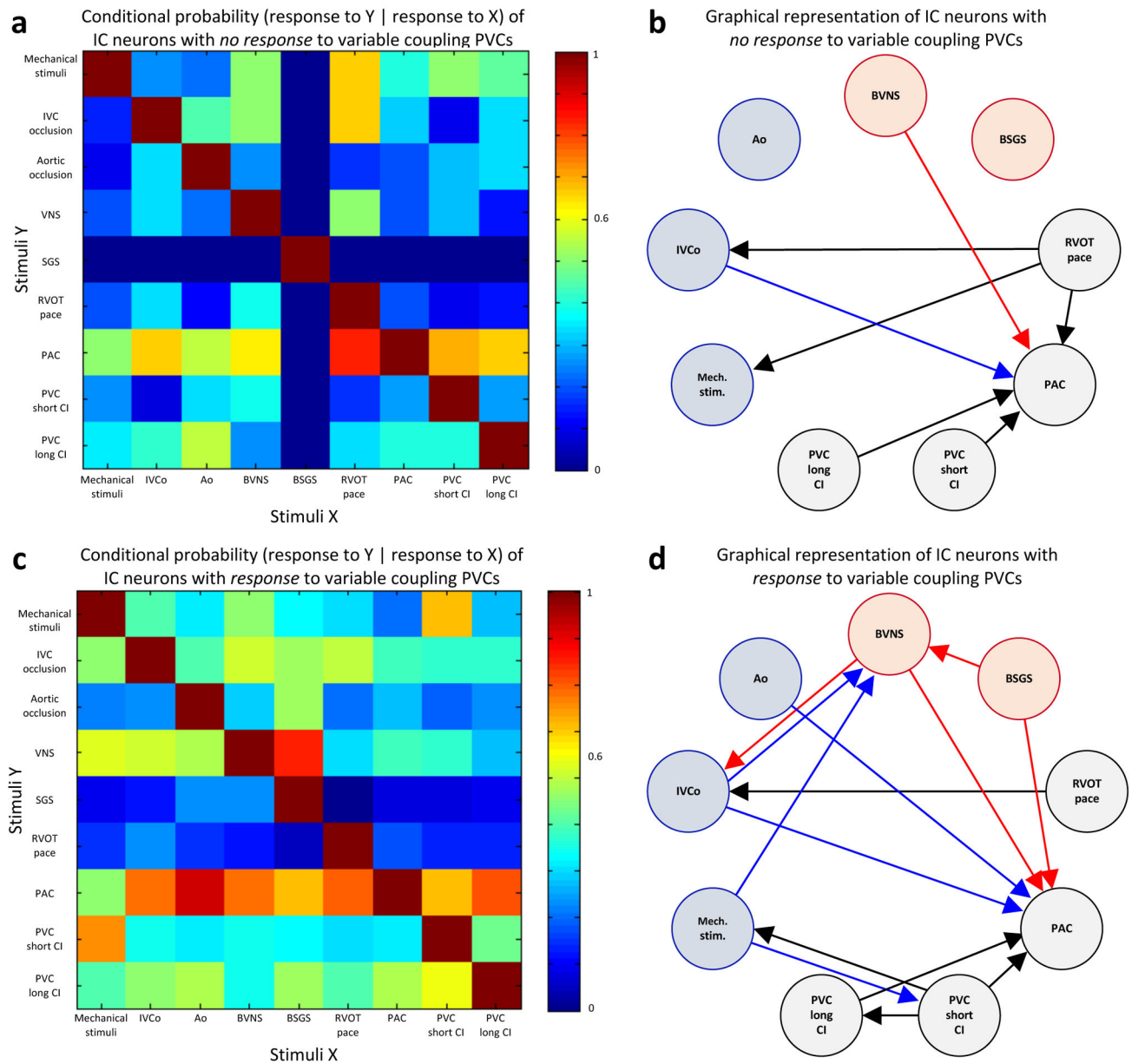


**Figure 6.** Impact of variable coupling interval PVCs on ICNS network function. **(A, C)** Conditional probability that an intrinsic cardiac neuron that responded to one stimulus (X, x-axis) also responded to another stimulus (Y, y-axis). Panel A shows conditional probability for neurons that had no response to variable coupling interval premature ventricular contractions (PVCs), and panel B shows that of neurons that had a response to variable coupling interval PVCs. Color scale indicates level of probability of each occurrence. **(B, D)** Graphical representation of interdependent interactions between stimuli in neurons based on their response to variable coupling interval PVCs (panel B, no response; panel D, response). Only links with probabilities  $\geq 0.6$  are displayed. Afferent and efferent stimuli are represented by blue and red, respectively. Pacing, premature atrial contractions (PACs) and PVC are

represented in black. Ao, aortic occlusion; BSGS, bilateral stellate ganglia stimulation; BVNS, bilateral vagus nerve stimulation; CI, coupling interval; IVCo, inferior vena cava occlusion; Mech., mechanical; RVOT, right ventricular outflow tract; stim., stimuli.

Author Manuscript

Author Manuscript

Author Manuscript

Author Manuscript

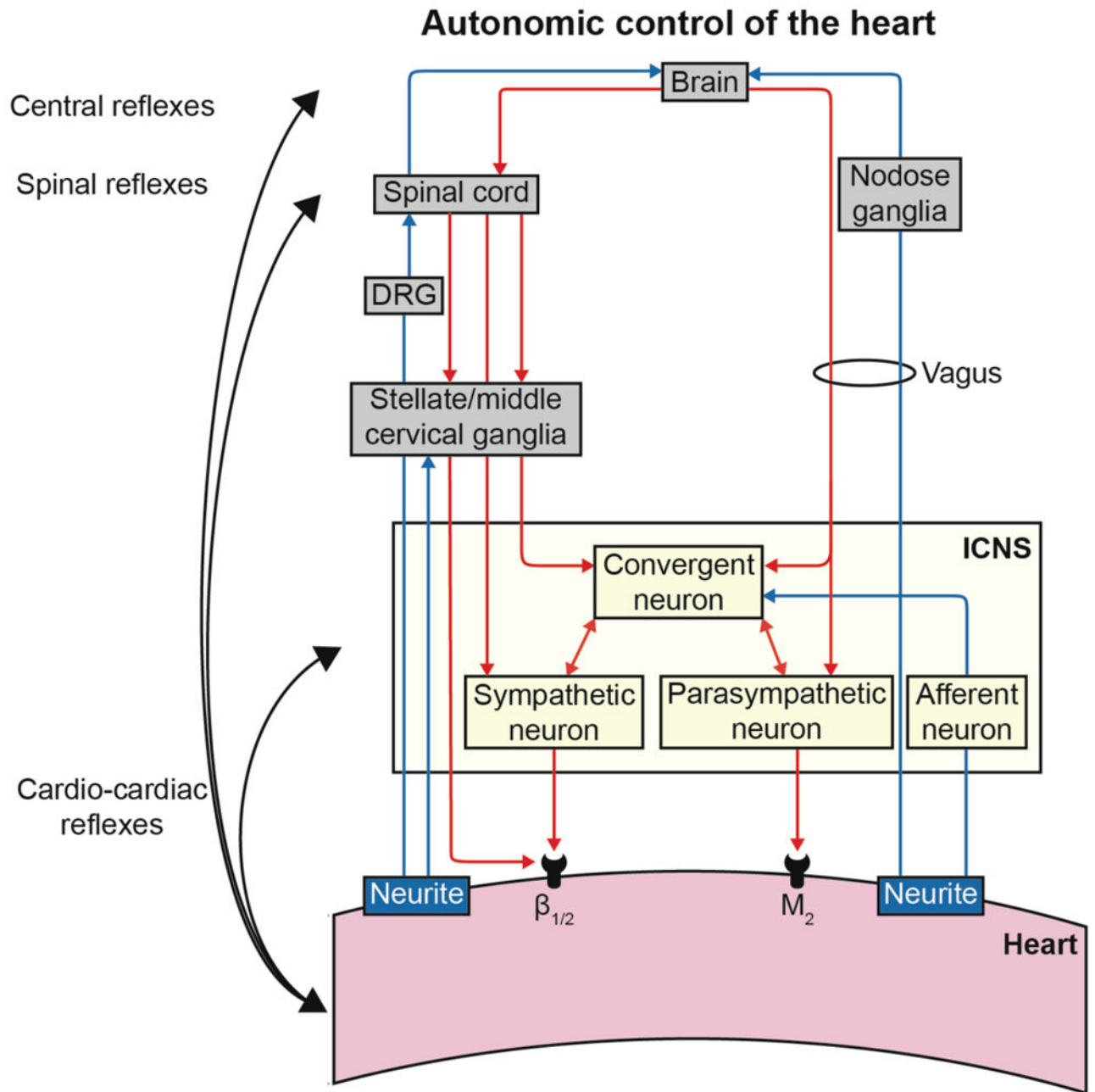


**Figure 7. Autonomic control of the heart**  
 DRG, dorsal root ganglia; ICNS, intrinsic cardiac nervous system.



**Table 1**

Hemodynamics of extrasystolic and post-extrasystolic sinus beat. **(A)** Left ventricular (LV) end-systolic pressure (LV ESP), maximum rate of LV pressure change (LV +dP/dt) and minimum rate of LV pressure change (LV -dP/dt) for ventricular and atrial extrasystolic (ES) beats of different coupling intervals. **(B)** Hemodynamic parameters of post-extrasystolic sinus beat (PES-SB) following ventricular and atrial ES beats of different coupling intervals.

ES	LV ESP (mmHg)	LV +dP/dt (mmHg/s)	LV -dP/dt (mmHg/s)
<b>PVC short coupling</b>	53 ± 13 *	488 ± 82 *	-520 ± 179 *
<b>PVC long coupling</b>	81 ± 11	1012 ± 139	-919 ± 180
<b>PAC short coupling</b>	66 ± 16	722 ± 180 *	-834 ± 271
<b>PAC long coupling</b>	83 ± 12	1072 ± 139	-1042 ± 162
<b>PES-SB</b>			
<b>PVC short coupling</b>	88 ± 12	1524 ± 179 †	-1040 ± 166
<b>PVC long coupling</b>	84 ± 11	1213 ± 150	-1058 ± 161
<b>PAC short coupling</b>	84 ± 14	1308 ± 203 *	-929 ± 220
<b>PAC long coupling</b>	85 ± 13	1207 ± 181	-991 ± 181

PAC, premature atrial contraction; PVC, premature ventricular contraction.

\*, P<0.05 for short versus long coupling.

†, P<0.001 for short versus long coupling.